Journal of the Serbian Chemical Society
JSCS@tmf.bg.ac.yu • www.shd.org.yu/JSCS

J. Serb. Chem. Soc. 72 (11) 1127–1138 (2007)
JSCS–3647

UDC 546.284–31.002.2:539.22:666.293.35
Original scientific paper

Fabrication of SiO_2-based microcantilevers by anisotropic chemical etching of (100) single crystal Si

VESNA JOVIĆ*#, JELENA LAMOVEC, MIRJANA POPOVIĆ# and ŽARKO LAZIĆ

Institute of Chemistry, Technology and Metallurgy – Center for microelectronic technologies and single crystals, Njegoševa 12, Belgrade, Serbia

(Received 19 July 2006)

Abstract: The undercutting process of thermal SiO_2 microcantilevers with different orientations on (100) Si wafer was studied. The silicon substrate was removed by anisotropic chemical etching with a 25 wt. % aqueous solution of TMAH or a 30 wt. % aqueous KOH solution at 80 °C. It was found that ⟨110⟩ oriented cantilevers were undercutting frontally along the length and ⟨100⟩ oriented cantilevers experience undercutting along the width of the cantilever, which is a less time consuming process. The studies showed that the ⟨100⟩ orientation of SiO_2 microbridges enables theirs fabrication on a (100) oriented Si substrate.

Keywords: anisotropic wet chemical etching, TMAH, KOH, SiO_2 microcantilever, SiO_2 microbridge, (100) oriented Si substrate.

INTRODUCTION

Since its discovery in the middle of the 1960s, anisotropic wet chemical etching[1] of single crystal silicon (sc Si) has been widely used in the semiconductor industry. Nowadays this technique is applied in the fabrication of different types of sensors and actuators and optical components in micro-electro-mechanical-system (MEMS) technologies.[2]

Microcantilevers and microbridges are one of the major diagnostic structures not only in a variety of sensors,[3] but also for measuring mechanical (*e.g.* residual stress and Young's modules)[4] or thermal (*e.g.* thermal expansion coefficients)[5] properties of thin films used in MEMS technologies.

This paper describes the experimental results used to investigate the correlation between the orientation of the microcantilevers and microbridges after anisotropic wet etching of silicon substrates. In the fabrication of SiO_2 microcantilevers or microbridges, anisotropic wet etching of Si substrate beneath the SiO_2 film creates free standing structures. Silicon dioxide is relatively insoluble in aque-

* Corresponding author. E-mail: vjovic@nanosys.ihtm.bg.ac.yu
# Serbian Chemical Society member.
doi: 10.2998/JSC0711127J

ous alkaline solutions of TMAH (tetramethylammonium hydroxide) or KOH which are used for anisotropic etching.[2] SiO_2 thin films are transparent which enables the observation of the Si undercut processes during etching. Conclusions about the anisotropic etching of sc Si substrates could be useful in etching microcantilevers made from opaque materials insoluble in these solutions. Also, many SiO_2-based microcantilever systems are successfully designed and fabricated for various MEMS applications.[6,7] Hence, the main aim of this work was to establish the conditions for Si substrate undercutting during the course of etching and find the optimal orientation of the released microcantilevers and microbridges.

EXPERIMENTAL

The SiO_2 microcantilevers used for these experiments had been fabricated on n-type (boron-doped) sc Si wafers with the (100) orientation. The Si wafers were mirror polished and has resistivity values between 5 and 3 Ω cm. Approximately 1 μm thermal oxide was grown on the Si substrate in oxygen ambient saturated with H_2O vapor. The temperature for the silicon oxide growth was 1115 °C. Designed structures were patterned using a standard photolithographic technique[8] and openings in the SiO_2 were etched using a buffer oxide etch. The cantilevers patterns were aligned to the prime wafer flat on the (100) Si substrate, *i.e.*, along the ⟨110⟩ direction. Two types of cantilevers and microbridges orientations were investigated: one parallel to the prime flat or aligned to the ⟨110⟩ direction and the other was oriented to the ⟨100⟩ direction, which is 45° from the prime wafer flat. The dimensions of the designed cantilevers and microbridges were 25, 50 or 100 μm in width and 100, 200, 300 or 500 μm in length.

The etching process was carried out using two alkaline solutions which are the most frequently used in MEMS processing, namely: a 25 wt. % aqueous TMAH solution or a 30 wt. % aqueous KOH solution. The solutions are held in a thermostated Pyrex glass vessel at the etching temperature of 80 °C (temperature stabilization ±0.5 °C) for both solutions. The vessel was sealed with a screw on lid which included a tap water cooled condenser, to minimize evaporation during the etching. During the etching, the wafer was held in a Teflon holder in the horizontal position above a magnetic stirrer bar. The solution was electromagnetically stirred at 700 rpm. A detailed description of the apparatus is given in the literature.[9]

After the etching process, the etched wafers were removed from the solution and thoroughly rinsed with deionized water without the application of any procedure[10] for the prevention of cracking or stiction of the released microcantilevers. In future work with the aim of fabricating microcantilevers for specific application, drying and stiction problems should be resolved because they are directly connected with yield of fabricated devices.

The released structures were subjected to microscopic observations using a high power optical microscope “Epival Interphako”, Carl Zeiss, Germany, which allows for longitudinal in plane measurement. To estimate the etch rates of the examined crystal planes, the depth of etching was measured using a special micrometric gauge.

RESULTS AND DISCUSSION

It is well known that Si has a diamond cubic structure and its anisotropic etching behavior strongly depends on the crystal orientation.[2] The family of {100} planes in silicon posses four fold symmetry and their anisotropic etching can produce either vertical {100} walls or sloping {110} or {111} walls, inclined at 45° or 54.7°, respectively.[11] Plane formation of a sidewall during anisotropic wet chemical etching is the one with the slowest etch rate aligned to the mask edge. All these possibilities are shown in Fig. 1.

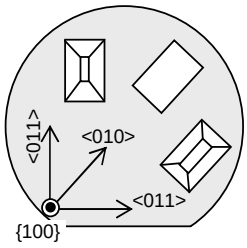

Fig. 1. Different structure types which can be produced by anisotropic etching on a (100) Si substrate. Gray field represents the masking material (SiO_2).

To achieve {111} walls, the pattern edges must be in the ⟨110⟩ direction, which is also the direction of the prime flat in (100) Si wafers. {111} Planes are the slowest etching planes in both the solutions examined in this work.

When the pattern edge is aligned along the ⟨100⟩ direction, *i.e.*, 45° from the prime flat, the selection of walls bounded pattern depends on relative etch rates of the {110} and {100} planes. There is small difference between these two etch rates and they are very sensitive toward the employed solution, etching conditions, temperature, additives, impurities in solution, *etc*.

The method of evaluation of the etching rates of some crystallographic plane is illustrated in Fig. 2. The etched depths (*d*) on Si (100) substrate were measured using a micrometer gauge and the lateral distances were measured under an optical microscope.

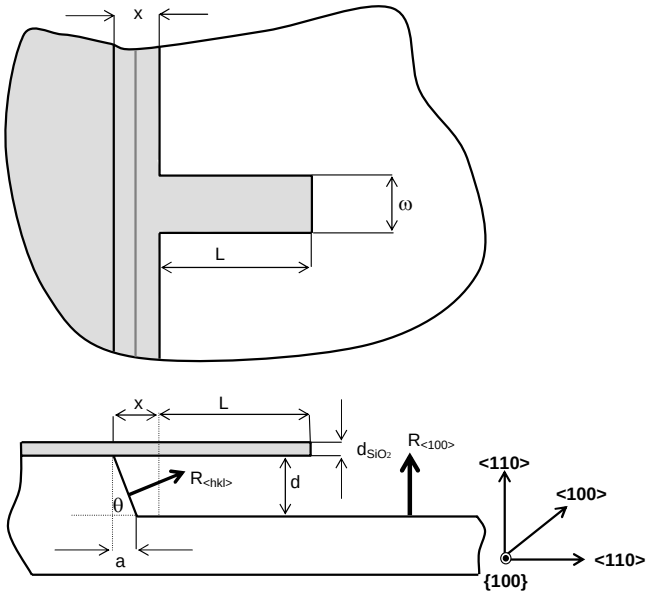

Fig. 2. The method for estimating the etch rate of Si crystallographic planes. A SiO_2 microcantilever is released by undercutting of the Si substrate.

By measuring the etching depth (*d*) in the ⟨100⟩ direction and knowing the etching time (τ), the etch rate of the (100) plane, $R_{\langle 100\rangle}$, is calculated from the Equation:

$$R_{\langle 100\rangle} = d\,\tau^{-1} \tag{1}$$

By measuring the distance a, which is the side wall projection on the (100) surface, the angle of inclination, θ, of the developed plane toward the (100) substrate surface can be estimated as:

$$\theta = \text{arctg}\,\frac{d}{a} \tag{2}$$

This angle determines unambiguously which crystallographic plane has developed in the considered crystal direction. The etch rate of a developed sloped plane with {hkl} orientation can be estimated from the formula:

$$R_{\langle hkl\rangle} = \frac{x \sin\theta}{\tau} \tag{3}$$

where x is the undercutting of the oxide mask. It is important to notice that x denotes not only the undercutting of the oxide mask, but also the distance which defines how ideally the microcantilever is clamped. For ideally clamped microcantilevers, $x = 0$.

By measuring the etching depth in the ⟨100⟩ direction for a given etching time, it is possible to determine the etching rate (Eq. (1)) of the (100) planes in both solutions. Etching rates are 0.44 μm min^{-1} for the 25 wt. % aqueous TMAH solution at 80 °C and 1.30 μm min^{-1} for the 30 wt. % aqueous KOH solution at 80 °C. The etching rate of the sloped {111} planes were determined in both solutions using Eq. (3), knowing the slope angle ($\theta = 54.7°$) and measuring x for a given etching time. The determined etching rates of the {111} planes are 2.2×10^{-2} and 5.0×10^{-3} μm min^{-1} for the TMAH and KOH solution, respectively.

The etching rates experimentally determined in this work are in agreement with those reported in the literature.[11]

The photographs in Fig. 3 display the undercut process of various microcantilevers oriented in the ⟨110⟩ direction on a (100) Si wafer. The photographs were obtained using the optical microscope (OM) working in reflected light. The microcantilevers of different widths and lengths were etched in a 25 wt. % aqueous TMAH solution for two different etching times. These photographs illustrate the Si undercutting process and the release of SiO_2 microcantilevers. The lateral sides of the microcantilevers are bounded with the slowest etching {111} planes and the release process was practically performed by undercutting of the convex-corners at the top of the microcantilever.

The successive steps during undercutting of the substrate below the masking material are schematically presented in Fig. 4. The dashed lines are traces of Si planes in the (100) substrate during the course of undercutting. For microcantilevers oriented in the ⟨110⟩ direction, the general picture of Si undercutting was similar for both applied solutions (*i.e.*, TMAH and KOH).

This is well illustrated for etching in 30 wt. % KOH solution in Fig. 5. The OM photographs of microcantilevers oriented in the ⟨110⟩ directions are shown in

Fig. 5a after their etching for 30 min. in the KOH solution. Completely released SiO_2 microcantilevers of 200 μm length but of different widths are shown in Fig. 5b.

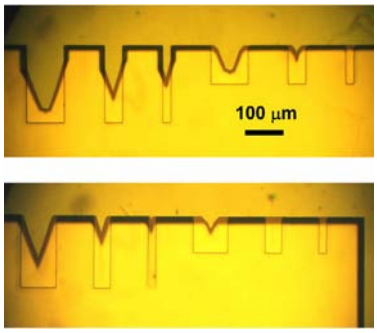

Fig. 3. OM Photographs of the microcantilevers undercut process in 25 wt. % TMAH solution on (100) Si wafers when the etching time was 0.75 h (top) and 1.25 h (bottom). The microcantilevers were oriented in the ⟨110⟩ direction.

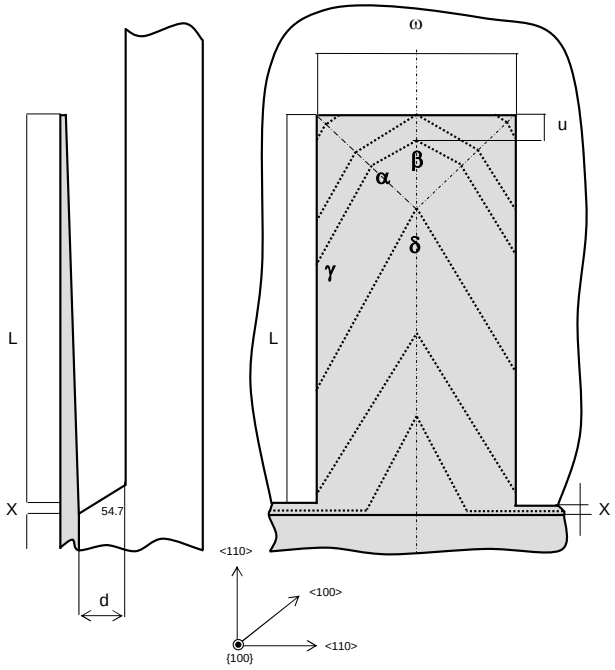

Fig. 4. Schematic presentation showing the evolution of an undercutting configuration of ⟨110⟩ orientted microcantilevers, which results in their release.

From the evolution of Si undercutting during the release of ⟨110⟩ oriented microcantilevers, it can be seen that {111} crystallographic planes stop the undercut from the edge of the microcantilevers. Hence, for ⟨110⟩ oriented microcantilevers the undercutting results from the convex corner effect, this spreads along the cantilever length. The undercutting mechanism was the same in both solution, and only difference lay in type of the fastest etching planes which bound the convex corners at the fronts of the microcantilevers. This means that the angles shown in Fig. 4 are different for each solution. Details of the values of the angles from Fig. 4 for both solutions are compiled in Table I. Traces in the (100) substrate of

the fastest etching planes, the undercutting of which determines the undercutting of the convex corner,[2,13] are given in Table I.

(a)

(b)

Fig. 5. OM Photographs of ⟨110⟩ oriented microcantilevers released by wet chemical etching in 30 wt. % aqueous KOH solution: (a) etching time 30 min, (b) completely released SiO_2 microcantilever. The released SiO_2 microcantilever shows color variations due to the change in thickness as a result of chemical dissolution in the used solution.

TABLE I. Numerical values of the angles characterizing the undercutting of the substrate for ⟨110⟩ oriented microcantilevers on (100) Si substrate for etching in KOH and TMAH solutions at the temperature of 80 °C (according to the sketch in Fig. 4)

Angle	30 wt. % KOH	25 wt. % TMAH
	{410}	{520}
α / °	152	136.4
β / °	118	133.6
δ / °	62	46.5
γ / °	149	156.8

Knowledge of the exact orientation of the planes binding the convex corner of Si is very important when the microcantilever is made from silicon itself. In this case, undercutting of the convex corners must be avoided in order for the microcantilever to maintain its predetermined shape.[14]

The schematic presentation in Fig. 3 shows a cross-section of a released SiO_2 microcantilever along its longer axis, from which it can be seen that there is continuous thickness change. The change in the thickness of a microcantilever is more pronounced when the etch rate of the material (SiO_2 in this case) is higher. The geometry (especially thickness) of a microcantilever is a key factor for the accuracy of a measurement when microcantilevers are applied as measurement or diagnostic devices.[15]

By measuring the height of the SiO_2 steps after etching, the etching rates of cantilever's material were estimated as: 0.13 nm min^{-1} in the TMAH solution (25 wt. %, 80 °C) and 7.3 nm min^{-1} in the KOH solution (30 wt. %, 80 °C). Thus SiO_2 is much more stable in the TMAH solution, which is well illustrated in Fig. 5b. The completely released microcantilevers in this photograph show a variety colors, which is the outcome of the different thickness of the SiO_2. Such

color changes were not observable for the SiO_2 microcantilevers released in the TMAH solution, which is quite understandable bearing in mind that the SiO_2 etch rate is approximately sixty times slower in TMAH than in KOH under the given etching conditions.

Sometimes, microcracks were observed during the etching of microcantilevers oriented along the ⟨110⟩ direction, as can be seen in Fig. 6a. In addition, some cantilevers broke along the microcracks (Fig. 6b). The appearance of cracks is due to the effect of stress concentration at the tip of the sharp corner shown in Fig. 4 (angle δ).

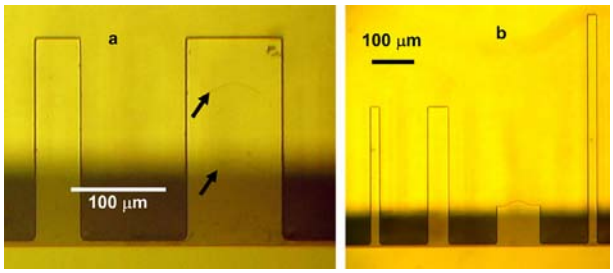

Fig. 6. MO Photographs of (a) ⟨110⟩ oriented SiO_2 microcantilevers with microcracks on the wider one (marked with the arrows) and (b) the breakage of a microcantilever along a previously formed microcrack.

Concerning microcracks in SiO_2 microcantilevers, it must be born in mind that internal stress is unavoidable in thermally grown silicon dioxide.[16] Undoubtedly, the interference of these stresses facilitate cantilever breakage.

Knowledge of the etching time required to fabricate a cantilever with a given length (L) and width (ω) is very important. Every time a wafer with cantilevers has to be removed from the etching solution to control the completeness of undercutting, the probability for the cantilever to break or stick increases. As indicated by the dashed lines in Fig. 4, the undercut of a ⟨110⟩ oriented cantilever is along its length. This means that cantilevers of the same lengths are going to undercut for a longer time the broader they are. The measured results for undercutting Si substrate in ⟨110⟩ direction (u, in μm) in dependence of etching time (τ, in min) is shown in Figs. 7a and 7b, for the KOH solution and TMAH solution, respectively.

When the undercutting, u, equals to the length of cantilever (L), it is completely released. The sloped plane under the place where the microcantilever was clamped is a plane from the {111} family, the slowest etching plane in the examined solutions, thus $\theta = 54.7°$ (Fig. 2).

To release a SiO_2 microcantilever of 500 μm length and 25 μm width with a ⟨110⟩ orientation on a (100) Si substrate, 120 min etching in the KOH solution and 180 min etching in the TMAH solution were required. The etching depth of a (100) substrate (d in Fig. 2) was 79 μm for the TMAH solution and 156 μm for the KOH solution. The SiO_2 undercutting (denoted by x in Figs. 2 and 4 and calculated from Eq. (3)) for these etching times was 0.7 μm and 4.3 μm for etching in the KOH and TMAH solutions, respectively.

Considering SiO_2 microbridges as beams clamped at both ends, it can be seen that their fabrication for the ⟨110⟩ orientation on Si (100) substrates is impossible.

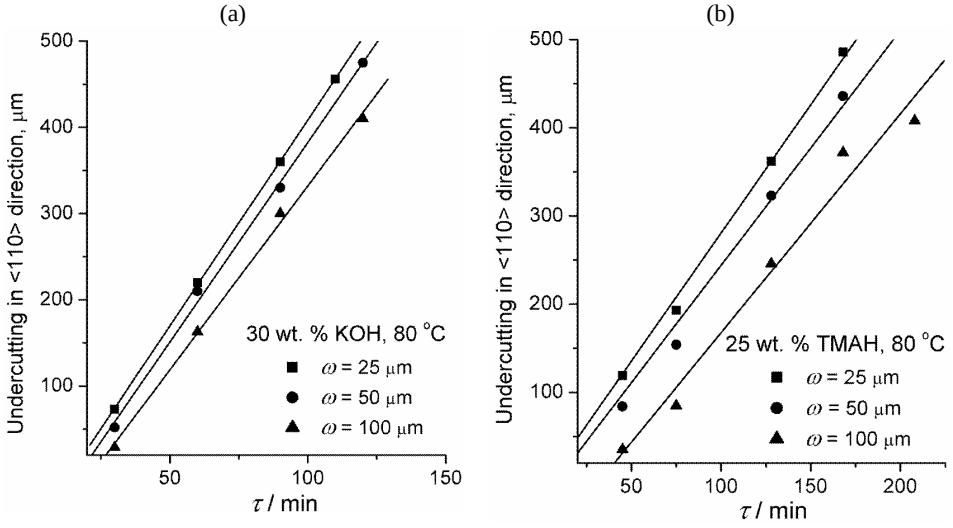

Fig. 7. The experimental relation between undercutting and etching time for ⟨110⟩ oriented SiO_2 cantilevers on a (100) Si substrate with different widths (ω). The cantilevers were released by anisotropic chemical etching in (a) 30 wt. % aqueous KOH solution and (b) 25 wt. % aqueous TMAH solution. The etching temperature was 80ºC.

Photographs from the optical microscope of microcantilevers oriented in the ⟨100⟩ direction on a Si (100) substrate (*i.e.*, 45° from the prime wafer flat) after etching in the TMAH solution and KOH solution are shown in Figs. 8 and 9, respectively.

From these photographs it is obvious that the release of ⟨100⟩ oriented SiO_2 microcantilevers on a (100) Si substrate occurs by undercutting of the substrate along the length of a microcantilever. At the very first moments of undercutting, the Si structure beneath the cantilever is bound by high index planes with the highest etch rates but as the etch time elapses, the dominant undercutting mechanism is lateral etching, as is schematically shown in Fig. 10.

This undercut process protects the cantilever from the formation of microcracks due to the stress concentration effect of the sharp corner. Also, the etching time required to fabricate a cantilever is independent of the cantilever length and depends only of its width. The cross-section of microcantilever is trapezium (Fig. 10) and the change of thickness is symmetrical about longitudinal axis of the microcantilever.

For ⟨100⟩ oriented microcantilevers fabricated by etching in the TMAH solution, the sloped plane underneath the clamp position is from the {110} family, hence the angle $\theta = 45°$ (Fig. 10). In the TMAH solution, under the given etching conditions, $R_{\langle 110\rangle} < R_{\langle 100\rangle}$, θ is determined from Eq. (2) by measuring the etching depth (d) of the Si substrate (in the ⟨100⟩ direction) and the length of the side-wall projection of this oblique plane on the (100) substrate surface (a). The etching rate

of the {110} planes was calculated from Eq. (3) and the measured value of x, as $R_{\langle 110\rangle} = 0.32\ \mu m\ min^{-1}$.

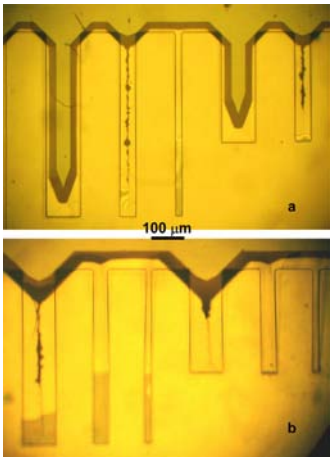

Fig. 8. OM Photographs of SiO_2 microcantilevers etched in a 25 wt. % aqueous TMAH solution at 80 °C. The microcantilevers are oriented in ⟨100⟩ direction on a (100) Si substrate. The etching time was: (a) 60 min. and (b) 120 min. It can be seen that some of the microcantilevers are stuck on the substrate.

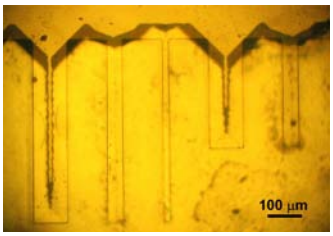

Fig. 9. OM Photographs of SiO_2 microcantilevers etched in a 30 wt. % KOH solution at 80 °C for 30 min. The microcantilevers are oriented in the ⟨100⟩ direction on a (100) Si substrate.

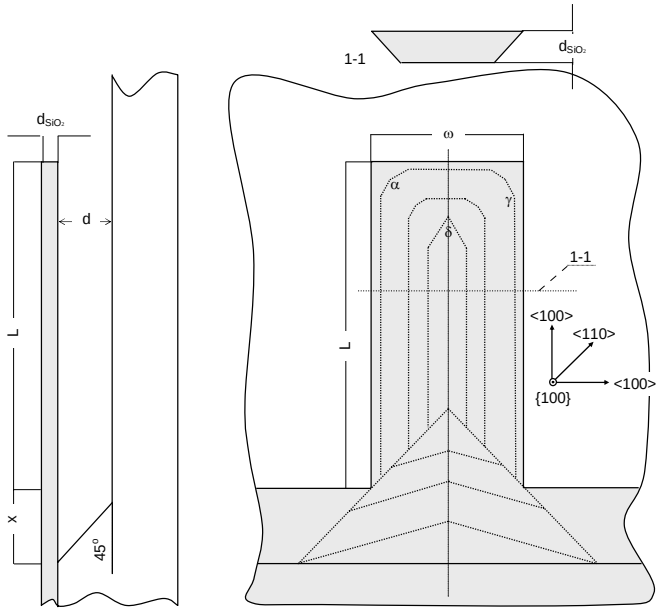

Fig. 10. Undercut process of a SiO_2 microcantilever oriented in the ⟨100⟩ direction on a (100) Si substrate.

For the etching of ⟨100⟩ oriented microcantilevers in the KOH solution, there is no sloping planes underneath the clamp positions because under these etching

conditions $R_{\langle 100\rangle} < R_{\langle 110\rangle}$. From Fig. 9 and the calculations from the measured values, it can be seen that $\theta = 90°$ (in Fig. 2).

The results shown in Fig. 11 indicate that the etching time for ⟨100⟩ oriented microcantilevers is smaller than for microcantilevers oriented in the ⟨110⟩ direction if they have same width and length. This is true for both examined solutions.

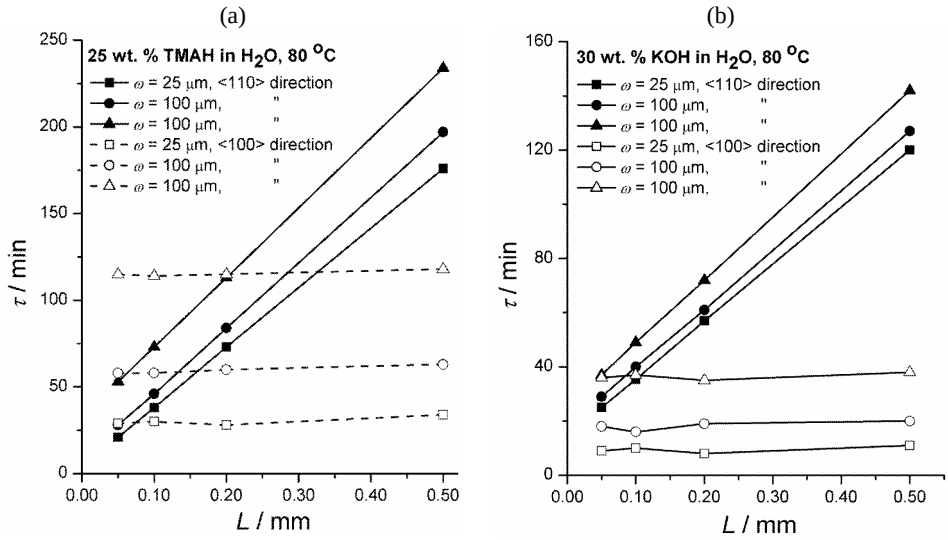

Fig. 11. The relation between beam length, L, and etching time, τ, for microcantilevers orientated in the ⟨110⟩ direction (black symbols) and the ⟨100⟩ direction (open symbols) on aSi (100) substrate for both employed etching solutions: (a) 25 wt. % aqueous TMAH solution and (b) 30 wt. % KOH solution at 80 °C.

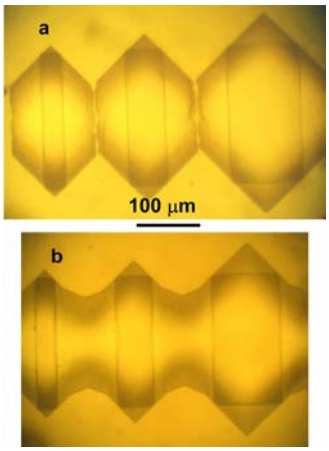

Fig. 12. SiO_2 microbridges oriented in the ⟨100⟩ direction on a (100) Si substrate which were (a) almost released by chemical etching in a 30 wt. % aqueous KOH solution and (b) completely released after etching in a 25 wt. % aqueous TMAH solution.

According to the undercut mechanism and the results shown in Fig. 11, the advantages of fabricating a microcantilevers with a ⟨100⟩ orientation over ones oriented in the ⟨110⟩ direction on a (100) Si substrate is the reduction of the etching time and the more appropriate cross-section of the cantilever for various applications.

Inspecting the SiO_2 microbridges oriented in the ⟨100⟩ direction in the Si (100) substrate, it is obvious that they could be released by wet chemical etching in these solutions, as is shown in Fig. 12.

CONCLUSIONS

This paper introduces some aspects of fabricating microcantilevers made from thermally grown SiO_2, with different orientation on Si (100) substrates. SiO_2 microcantilevers with either a ⟨110⟩ or ⟨100⟩ orientation were released by silicon undercutting in two solutions most often employed in micromachining technologies, namely 25 wt. % TMAH and 30 wt. % KOH aqueous solutions. The etching temperature was 80 °C for both solutions.

The ⟨110⟩ oriented microcantilevers are released by frontal undercutting and their etching time depends both on the width and length of the cantilevers. Also, such oriented microcantilevers exhibit thickness variation along their lengths and, due to the undercutting mechanism, are subject to microcrack development.

SiO_2 microcantilevers oriented in the ⟨110⟩ direction were fabricated by undercutting of the Si (100) substrate along theirs widths. The release of ⟨100⟩ oriented microcantilevers depends only of their widths and not on their lengths. The cross-section of SiO_2 microcantilevers oriented in such a way remains roughly rectangular, which is better for their further application.

It is possible to fabricate SiO_2 microbridges on a (100) oriented Si substrate by wet chemical etching only if they are oriented in the ⟨100⟩ direction.

*Acknowledgmen*t: This work was performed in the frame of the project “Micro and Nanosystems Technologies, Structures and Sensors”, supported by grants from the Ministry for Science of the Republic of Serbia, Grant No. TP-6151B.

И З В О Д

ИЗРАДА МИКРОГРЕДИЦА ОД SiO_2 АНИЗОТРОПНИМ ХЕМИЈСКИМ НАГРИЗАЊЕМ НА МОНОКРИСТАЛНОМ СИЛИЦИЈУМУ (100) ОРИЈЕНТАЦИЈЕ

ВЕСНА ЈОВИЋ, ЈЕЛЕНА ЛАМОВЕЦ, МИРЈАНА ПОПОВИЋ и ЖАРКО ЛАЗИЋ

Институт за хемију, технологију и металургију – Центар за микроелектронске технологије и монокристале, Његошева 12, Београд

Изучавана је реализација микрогредица од термички депонованог SiO_2 на монокристалним подлогама Si (100) оријентације. Гредице су реализоване анизотропним хемијским нагризањем у следећим воденим растворима: 25 теж. % ТМАН (тетраметиламонијум хидроксид) и 30 теж. % КОН. Температура нагризања је била 80 °C. SiO_2 микрогредице оријентисане у ⟨110⟩ правцу на Si (100) подлози се ослобађају чеоним подгризањем Si подлоге и брзина реализације гредице зависи и од њене ширине и од њене дужине. Утврђене су и брзине нагризања SiO_2 у овим растворима и показало се да промена дебљине гредице, која за овако оријентисане гредице постоји по дужини, бива израженија у растворима КОН. На SiO_2 микрогредицама ове оријентације је опажена појава микропрскотина које су објашњене самим механизмом подгризања Si у циљу “ослобађања” микрогредица ове оријентације. SiO_2 микрогредице оријентисане у ⟨110⟩ правцу на (100) Si подлози се “ослобађају” бочним подгри-

зањем Si подлоге и брзина њихове реализације не зависи од дужине микрогредице већ само од њене ширине. Микромостиће од термички депонованог SiO_2 је могуће реализовати анизотропним хемијским нагризањем у разматраним растворима само када су оријентисани у ⟨100⟩ правцу на (100) Si подлози.

(Примљено 19. јула 2006)

REFERENCES

1. K. E. Bean, *IEE Trans. Electrin devices* **ED-25** (1978) 1185
2. M. Madou, *Fundamentals of microfabrication*, CRC Press, Boca Raton, 1997, p. 145
3. N. V. Lavrik, M. J. Sepaniak, P. G. Datskos, *Review of Scientific Instruments* **75** (2004) 2229
4. Y. Zhang, Y.–P. Zhao, *Microsyst. Technol*. **12** (2006) 357
5. W. Fang, H.–C. Tsai, C.–Y. Lo, *Sens. Actuators* **A77** (1999) 21
6. Y. Tang, J. Fang, X. Yan, H.–F. Ji, *Sens. Actuators* **B97** (2004) 109
7. V. Chivukula, M. Wang, H.–F. Ji, A. Khaliq, J. Fang, K. Varahramyan, *Sens. Actuators* **A125** (2006) 526
8. S. Wolf, R. N. Tauber, *Silicon processing for the VLSI era*, Vol. 1, *Process technologies*, Lattice Press, Sunset Beach, California, 1986, p. 407
9. V. Jović, Ž. Lazić, M. Popović, *Proc. XLVII ETRAN Conference*, Čačak, June 6–10, IV, (2004), p. 164
10. C.–J. Kim, J. Y. Kim I, B. Sridharan, *Sens. Actuators* **A61** (1998) 17
11. O. Powell, H. B. Harrison, *J. Micromech. Microen.* **11** (2001) 217
12. E. Steinsland, T. Finstad, A. Hanneborg, *Sens. Actuators* **86** (2000) 73
13. V. Jović, Ž. Lazić, M. Popović, *ICOSECS 4*, Belgrade, July 18–21, Book of Abstracts, (2004), p. 119
14. K. Biswas, S. Das, S. Kal, *Microelectron. J*. **37** (2006) 765
15. A. W. McFarland, M. A. Poggi, L. A. Bottomley, J. S. Colton, *J. Micromech. Microeng*. **15** (2005) 785
16. A. Rawicz, M. Parameswaran, J. M. Chen, *Microelectron. Reliab*. **36** (1996) 1369.